Preparation and Characterization of Mn and Al co-doped Copper Oxide Films

An-Tian Du, Zhi-Peng San, Guang-Rui Gu, and Bao-Jia Wu

***Abstract*—In the present work, Mn and Al co-doped copper oxide (CuO-Mn:Al) thin films were deposited on Si(100) and ITO glass substrates by radio frequency (RF) and direct current (DC) magnetron co-sputtering, and then the obtained films were annealed at 800 ℃. The crystal structure of films was evaluated by X-ray diffraction. The surface morphology of films was observed by scanning electronic microscope (SEM). Elemental composition of films was determined by energy dispersive X-Ray diffraction (EDX) and X-ray photoelectron spectroscopy (XPS). The resistivity and optical band gap of CuO-Mn:Al thin films were determined by four probe resistance tester and ultraviolet visible near infrared (UV-Vis-NIR) spectrophotometer, respectively. XRD, EDX and XPS results show the perfect doping of Mn and Al into CuO host lattice. The addition of Mn:Al into copper oxide thin films led to the resistivity decreases. In contrast, the optical band gap values increased upon the addition of Mn:Al.**

***Index Terms*—Copper oxide films, electrical properties, magnetron co-sputtering, optical properties, surface morphology.**

I. Introduction

Copper oxides have been extensively studied because of their potential applications as solar cells [1]–[3], gas sensors [4], [5], electrochemical sensors [6], [7], and batteries [8], [9]. Copper oxides are also non-toxic, abundant, low cost, and easy to fabricate compared with other materials used for solar cells [10], [11]. The copper oxide mainly contains two kinds of structures: cupric oxide or tenorite (CuO) and cuprous oxide or cuprite (Cu_2O) [10]–[12]. A rarely reported copper oxide is paramelaconite (Cu_4O_3), which is an intermediate between Cu_2O and CuO [12], [13].

CuO has a preferred monoclinic structure, and its band gap ranges within 1.2eV-1.9eV [14]. CuO mostly possesses a direct band gap [2], [11], [13], although some studies have reported that CuO has an indirect band gap [14], [15]. The disparity in the findings of previous studies can be attributed to the complicated crystal structure of CuO and to the fact that CuO may belong to a particular class of compounds known as Mott insulators [16]. On the other hand, Cu_2O has a preferred cubic structure with a direct band gap ranging within 1.8eV-2.5eV [17], [18]. Both CuO and Cu_2O are p-type semiconductors that have the most stable defects in both Cu- and O-rich environments because of their copper vacancies. The band gap of copper oxides also strongly depends on the growth methods and parameters, as evidenced by the considerably discrepant values obtained by most researchers.

Numerous methods such as, reactive sputtering [17], [19]–[22], chemical vapor deposition [11], sol-gel [23], electro-deposition [24], and thermal oxidation [25], have been used to grow copper oxide thin films. Among these deposition methods, radio frequency (RF) sputtering is considered the best technique because of its advantage of proper stoichiometric control, low substrate heating during film deposition, and provision for uniform thickness on large-area substrates [12].

However, the research of the properties of metal-doped CuO films is rarely reported except for Al doping. The transition metal doped CuO films help to research the origin of ferromagnetism, on the other hand, it may produce excellent optical, electrical, magnetic and other electrical, which in solar cells and other aspects of a good application prospects.

In this work, Mn and Al co-doped Cu_xO (Cu_xO-Mn:Al) thin films were deposited on Si(100) and ITO glass substrates by RF and DC co-sputtering. The effects of doping on structure, electrical and optical properties of the obtained copper oxide thin films were investigated.

II. Experimental Details

The CuO-Mn:Al thin films were deposited on Si(100) and ITO glass substrates by RF and DC magnetron co-sputtering. Before the deposition, substrates were cleaned sequentially with acetone, ethanol and de-ionized water in an ultrasonic bath for 15 min each. The high purity (99.9%) Al target and Cu-Mn(9: 1) alloy target were used to co-sputter. The chamber was initially pumped to 5×10^{-4} Pa and the substrates were fixed on a rotating substrate holder at a distance of 60 mm above the target. The reactive sputtering conditions of the thin films are listed in Table I.

TABLE I: Reactive Sputtering Growth Conditions for the Metal-Doped Copper Oxide Thin Films (CuO-Mn:Al)

Experimental conditions	Cu-Mn target power (W)	Al target power (W)	Deposition pressure (Pa)	Ar-O_2 ratio	Al target sputtering time (min)
Si(100)	80	40, 50, 60	1.0	20:4	5, 10, 15
ITO glass	50	40, 50, 60	0.8	20:10	5, 10, 15

The crystal structure of films was characterized by X-ray

Manuscript received July 23, 2018; revised February 7, 2019. This work is supported by National Natural Science Foundation of China under Grants 51272224 and 11164031.

An-Tian Du and Guang-Rui Gu are with the Department of Physics, College of Science, Yanbian University, Yanji 133002, China (Corresponding author: Guang-Rui Gu; e-mail: 386757265@qq.com,.e-mail: grgu@ybu.edu.cn).

diffraction (XRD). The surface morphology of films was observed by scanning electronic microscope (SEM). Elemental composition of films was determined by energy dispersive X-ray (EDX) and X-ray photoelectron spectroscopy (XPS). The resistivity and optical band gap of metal-doped copper oxide thin films were determined by four probe resistance tester and ultraviolet visible near infrared spectrophotometer, respectively.

III. Results and Discussion

A. Structural Properties

Fig. 1 shows the XRD diffraction patterns of the CuO-Mn:Al films deposited on Si substrates at different doping power. For the film without metal addition, a single diffraction peak was observed and can be well indexed as (002) planes of CuO. With the addition of Mn into CuO films, a single diffraction peak (002) plane of CuO disappeared and a very weak peak at the position of 2θ =36.5 ° appeared, which was ascribed to the diffraction pattern from (002) plane of Cu_2O. With the addition of Al into CuO films, the diffraction peak intensity in the (002) plane of CuO was declined and the peak position was normal. It indicated that Al ions were doped into the lattice of CuO and it was not certain whether or not to occupy the vacancy of the body. With further increase of Al doping power, the intensity of CuO (002) peak increases gradually, while the crystallinity of the film is improved. When the Al doping power is 40W, the diffraction peaks of Cu_2O (111) plane and Cu_2O (200) plane appear and the diffraction peak of Cu_2O disappears as the power further increases. Therefore, metal doping has a significant effect on the film structure [26].

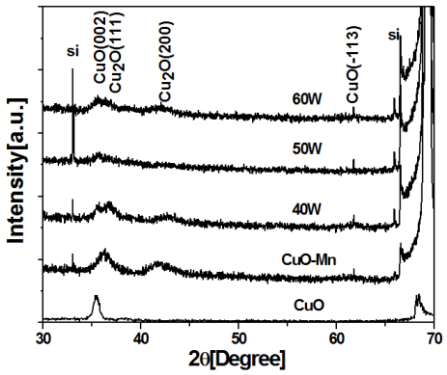

Fig. 1. XRD patterns of CuO-Mn: Al films deposited on Si substrates at different doping powers.

Fig. 2 shows the XRD diffraction patterns of the CuO-Mn: Al films deposited on ITO glass substrates at different doping power. It can be seen from Fig. 2 that the XRD diffraction patterns change very slightly with Al doping power increases. With the addition of Mn into CuO films, a very slightly shift of the CuO (002) diffraction peak was observed. It indicated that Mn was successfully doped into the CuO lattice. With the addition of Al into CuO films, a diffraction peak (111) plane of CuO appeared. From the XRD patterns with Si and ITO glass substrates, it can be seen that two substrates present different effect as the Al doping power changes. It shows that different substrates have a significant effect on the film structure [26].

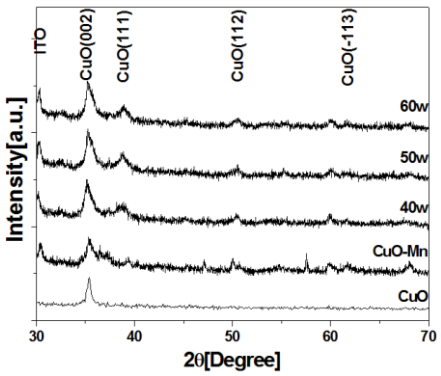

Fig. 2. XRD patterns of CuO-Mn: Al films deposited on ITO glass substrates at different doping power.

Fig. 3 shows the XRD diffraction patterns of the CuO-Mn:Al films deposited on Si substrates at different doping time. It can be seen from Fig. 3 that the XRD diffraction patterns change very slightly with doping time increases. A diffraction peak (002) plane of the CuO film deposited at the doping time of 15 min disappears almost and therefore as-deposited films are almost amorphous. It could be ascribed to Al and Mn ions are doped into the CuO unit cell and the CuO crystal quality was reduced [27].

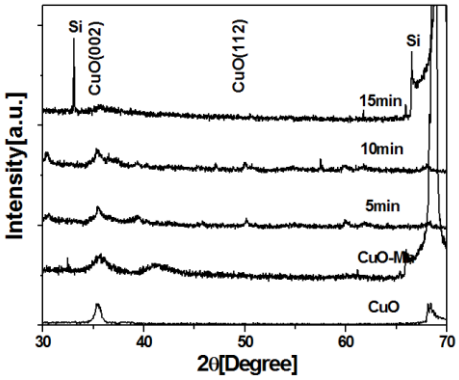

Fig. 3. XRD patterns of CuO-Mn: Al films deposited on Si substrates at different doping time.

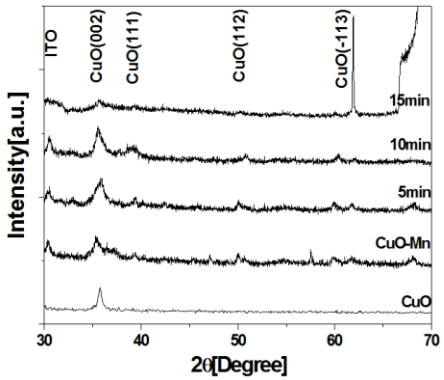

Fig. 4. XRD patterns of CuO-Mn: Al thin films deposited on ITO glass substrates at different doping time.

Fig. 4 shows the XRD diffraction patterns of the CuO-Mn:Al films deposited on ITO glass substrates at different doping time. With the doping time increasing, the diffraction peak intensity of the (002) plane of CuO films is increased slightly at first and then decreased. The diffraction peak (-113) plane of the CuO film deposited at the doping time of 15 min appears evidently. The increase of doping

time results in the increase of Al content. It is clear from the XRD patterns that metal doping can change the crystallographic structure. It can be observed clearly the decrease in the (002) peak intensity and increase in the (-113) peak intensity. Further, it is indicated that Al ions and Mn ions have been doped into the lattice of CuO. Thus, it is figured out that different substrates have a significant effect on the film structure.

XRD patterns of annealed CuO-Mn:Al films deposited on Si substrates at different doping power are shown in Fig. 5, and the annealed temperatures were 800 ℃. As shown in this figure, there is a distinct increase of the diffraction peak was observed for the Mn-doped films annealed at temperatures 800 ℃. The diffraction peaks in the (110) and (111) plane of CuO are formed. With the addition of Al into CuO:Mn films, the diffraction peak intensity in the (002) and (111) plane of CuO films is decreased, the diffraction peak in the (110) plane of CuO films is disappeared and the diffraction peak in the (-113) plane of CuO films is increased slightly. When, the diffraction peak intensity in the (002) and (111) plane of the CuO film deposited at the Al doping power of 60W is clearly increased. And the intensity of the CuO-Mn:Al film is higher than the CuO:Mn film. It can be seen that the crystallinity of the films has been improved. It may be attributed to the decrease of oxygen vacancy and Cu atoms defects. The observed decrease of the diffraction peak intensity can be due to the inducing thermal effect accompanied with recrystallization or reorientation of smaller grains to bigger one through crystal growth [28]–[30].

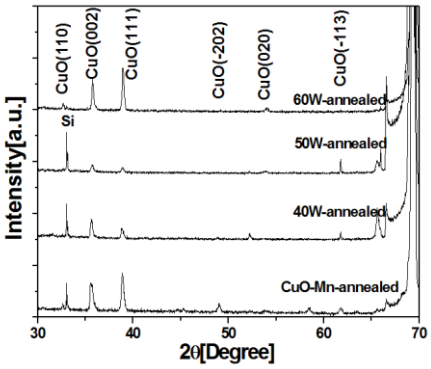

Fig. 5. XRD patterns of CuO-Mn: Al films after annealing deposited on Si substrates at different doping power.

TABLE II: THE LATTICE CONSTANT AFTER ANNEALING OF CUO-MN:AL THIN FILMS DEPOSITED ON SI SUBSTRATE BY DIFFERENT DOPING POWER

Samples	CuO	CuO-Mn-an	CuO-Mn:Al-an40W)	CuO-Mn:Al-an(50W)	CuO-Mn:Al-an(60W)
a (Å)	4.685	4.692	4.703	4.689	4.689
b (Å)	3.430	3.406	3.429	3.417	3.398
c (Å)	5.139	5.113	5.107	5.093	5.087

The copper oxide monoclinic lattice parameters *a*, *b*, *c* are obtained by using the relation:

$$\frac{1}{d^2}=\frac{1}{\sin^2\beta}\left(\frac{h^2}{a^2}+\frac{k^2}{b^2}\sin^2\beta+\frac{l^2}{c^2}-\frac{2hl\cos\beta}{ac}\right) \quad (1)$$

The calculated values of *a*, *b*, *c* are listed in Table II. These results are in accordance with literature reports [31]. As shown in Table II, there are slight changes in lattice constant for the films with different Al doping after annealing. The change of lattice constants can cause the modification of electronic band structure [32]. It is clear from the Table II that Al doping does not change the crystallographic structure evidently which is because ionic radii of Al (0.51 Å) is smaller than Mn and Cu [33].

B. Surface Morphology and Composition Analysis

Fig. 6 shows SEM images from CuO-Mn:Al films deposited at different doping power. Fig. 7 shows the corresponding EDX spectra. The deposited CuO-Mn:Al thin films exhibit approximate pyramid morphology change to the rugby form. The grain sizes decreases resulting in decreasing surface roughness. Therefore, the crystallinity of the film is poor. This consists well with the above XRD analysis results. The SEM images indicate that the surface morphology is strongly dependent on the metal-doped. The EDX images indicated that Mn was substantially retained. It can be ascribed to the use of synthetic targets. No Al element is found, which may be due to less content.

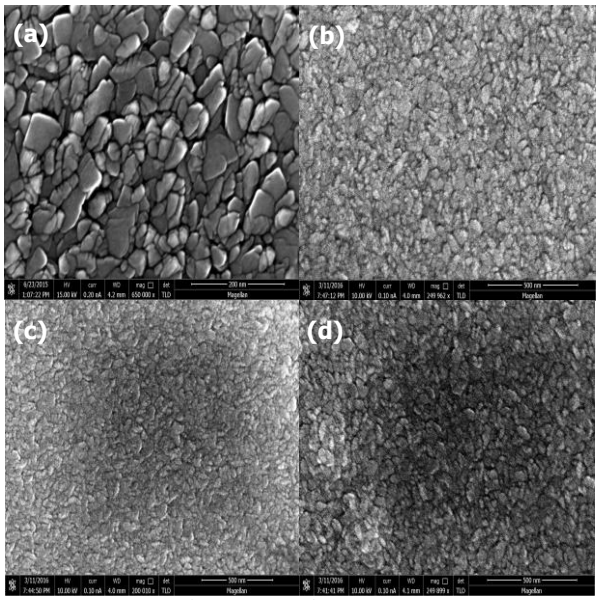

Fig. 6. SEM spectra of CuO-Mn:Al films deposited on Si substrates at different doping power; (a) undoped; (b) 40W; (c) 50W; (d) 60W.

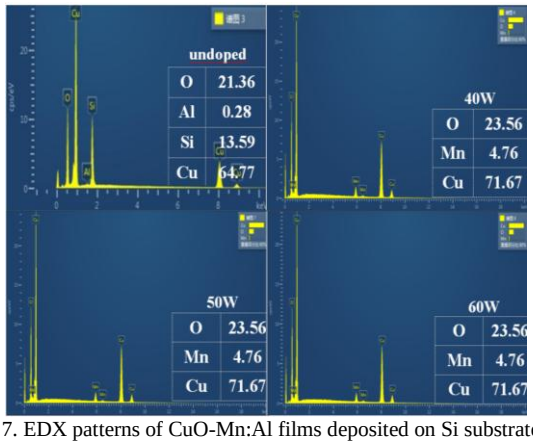

Fig. 7. EDX patterns of CuO-Mn:Al films deposited on Si substrates at different doping power.

In order to further clarify the phase composition of CuO-Mn:Al, X-ray photoelectron spectroscopy (XPS) was carried

out. Fig. 8 shows the XPS spectrum of CuO-Mn:Al films on Si substrates. A peak at about 76.3eV is assigned to $Al^{3+}2p_{1/2}$. This is similar to the results reported by Gong et al. [33]. It is shown that the aluminum in the film is almost completely in the form of Al^{3+}, which indicates that Al has successfully doped into the CuO lattice.

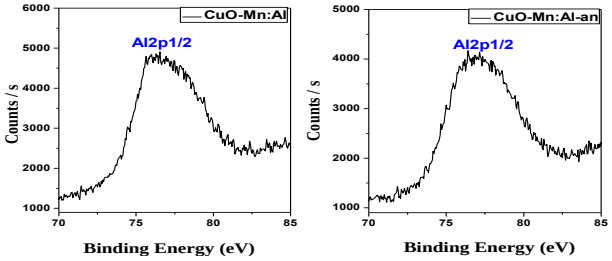

Fig. 8. XPS spectrum of CuO-Mn:Al films deposited on Si substrates.

C. Electrical Properties

Table III shows the variations in electrical resistivity as a function of doping time and power, respectively. It can be seen in Table III that the resistivity of the thin films deposited on the Si substrates increases with doping time increasing. The resistivity of the thin films deposited on the Si substrates decreases with doping power increasing. However, the resistivity of the thin films deposited on the ITO glass substrates decreases with doping time increasing. The resistivity of the thin films deposited on the ITO glass substrates increases with doping power increasing. Thus, it is figured out that different substrates have a significant effect on the film electrical properties. It is attributed to the change in free carrier concentration and mobility due to the change of film crystallinity. When the film crystallinity is improved, the internal defects in the film are reduced. The crystal quality of films plays a critical effect in the electrical properties. The resistivity of the films obtained in this work is much smaller than the reported results [34], [35].

TABLE III: RESISTIVITY IN CUO-MN:AL FILMS AS A FUNCTION OF DOPING TIME AND POWER, RESPECTIVELY

	Doping time(min)			Doping power(W)		
	5	10	15	40	50	60
Si substrate (Ω cm)	2.03	5.18	5.63	5.63	5.39	3.14
ITO glass substrates (Ω cm)	2.54	1.07	0.93	0.39	0.41	0.49

D. Optical Properties

In order to further investigate the optical properties of the films, the optical band gap of metal-doped copper oxide thin films were determined by ultraviolet visible near infrared (UV-Vis-NIR) spectrophotometer. The optical transmission spectra of films with different doping power are presented in Fig. 9. It can be seen that the transmittance distinctly decreases with Al doping in the visible range from 300 to 720nm. Excessive Al doping causes the movement of the band gap. An energy band widening (blue shift) effect is resulting from the increase of the Fermi level in the conduction band of degenerate semiconductors. It shows that the transmittance in the 1075nm and 1331nm is 34.8% and 36.2%, respectively. Subsequently, the optical band gap of the films is estimated using Tauc relationship:

$$(\alpha h\nu)^{\frac{1}{2}} = A(h\nu\text{-}Eg) \quad (2)$$

where A is a constant, α is the absorption coefficient, hυ is the photon energy, and E_g is the band gap. The band gap energy E_g can be determined by plotting α^2 versus hυ and extrapolating the linear part of the curve until it crosses the hυ axis where α^2 becomes zero. Fig. 10 shows the variation of α^2 as a function of hυ for doping power.

The band gap value obtained for undoped films is 2.84eV which is close to the reported value previously [26]. It shows that the band gap at the 40w, 50w and 60w is 3.57eV, 3.69eV and 3.63eV, respectively. According to Fig. 10, the band gap increase distinctly with the doping power increases. The increase of band gap with different doping power may be the result of changes in atomic distances which affects the band gap. This is attributed to the Mn and Al ions doped into the CuO lattice. This is consistent with the reported results [36], [37].

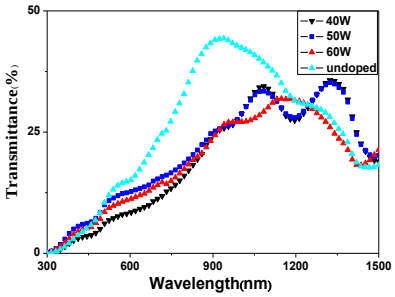

Fig. 9. Transmission spectra of CuO-Mn:Al films deposited on ITO glass substrates at different doping power.

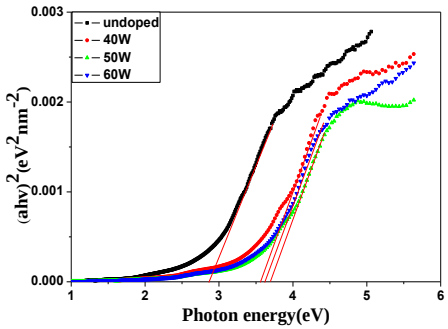

Fig. 10. Variation of α^2 as a function of photon energy for films deposited at different doping power.

IV. CONCLUSION

Mn and Al co-doped copper oxide (CuO-Mn:Al) thin films were deposited on Si(100) and ITO glass substrates by radio frequency (RF) and DC reactive co-sputtering. With doping time and power increasing, the crystallinity of the films changes. XRD, EDX and XPS results show the perfect solubility of doping Mn and Al into CuO host lattice. We have found that different substrates have a significant effect on the film structure. The transmittance distinctly decreases for CuO-Mn:Al films in the visible range from 300 to 720nm. The addition of Mn:Al into copper oxide thin films leads to the resistivity decrease. In contrast, the optical band gap values increased upon the addition of Mn:Al.

REFERENCES

[1] M. E. Salza, F. Sarto, M. Tucci, and R. Vasanthi, "Heterojunction solar cell with 2% efficiency based on a Cu_2O substrate," *Appl. Phys. Lett.*, vol. 88, 2006.

[2] R. Motoyoshi, T. Oku, H. Kidowaki, A. Suzuki, K. Kikuchi, S. Kikuchi, B. Jeyadevan, and J. Ceram, "Structure and photovoltaic activity of cupric oxide-based thin film solar cells," *Soc. Jpn.*, vol. 118, pp. 1021-1023, 2010.

[3] A. S. Zoolfakar, R. A. Rani, A. J. Morfa, S. Balendhran, A. P. O'Mullane, S. Zhuiykov, and K. Kalantar-zadeh, "Enhancing the current density of electrodeposited ZnO-Cu_2O solar cells by engineering their heterointerfaces," *J. Mater. Chem.*, vol. 22, pp. 21767-21775, 2012.

[4] C. Yang, X. Su, F. Xiao, J. Jian, and J. Wang, "Gas sensing properties of CuO nanorods synthesized by a microwave-assisted hydrothermal method," *Sens. Actuators B*, vol. 158, pp. 299-303, 2011.

[5] A. Chapelle, M. H. Yaacob, I. Pasquet, L. Presmanes, A. Barnabé, P. Tailhades, J. D. Plessis, and K. Kalantar-zadeh, "Structural and gas-sensing properties of CuO–$CuxFe_3$−xO_4 nanostructured thin films," *Sens. Actuators B*, vol. 1153, pp. 117-124, 2011.

[6] S. Zhuiykov, E. Kats, D. Marney, and K. Kalantar-zadeh, "Improved antifouling resistance of electrochemical water quality sensors based on Cu_2O-doped RuO_2 sensing electrode," *Prog. Org. Coat.*, vol. 170, 2011, pp. 67-73.

[7] S. Zhuiykov, E. Kats, K. Kalantar-zadeh, M. Breedon, and N. Miura, "Influence of thickness of sub-micron Cu_2O-doped RuO_2 electrode on sensing performance of planar electrochemical pH sensors," *Mater. Lett.*, vol. 175, pp. 165-168, 2012.

[8] Y. J. Mai, X. L. Wang, J. Y. Xiang, Y. Q. Qiao, D. Zhang, C. D. Gu, and J. P. Tu, "CuO/graphene composite as anode materials for lithium-ion batteries," *Electrochim. Acta*, vol. 156, pp. 2306-2311, 2011.

[9] Z. Wang, F. Su, S. Madhavi, and X. W. Lou, "CuO nanostructures supported on Cu substrate as integrated electrodes for highly reversible lithium storage," *Nanoscale*, vol. 13, pp. 1618-1623, 2011.

[10] A. Y. Oral, E. Menşur, M. H. Aslan, and E. Başaran, "The preparation of copper(II) oxide thin films and the study of their microstructures and optical properties," *Mater. Chem. Phys.*, vol. 183, pp. 140-144, 2004.

[11] T. Maruyama, "Copper oxide thin films prepared by chemical vapor deposition from copper dipivaloylmethanate," *Sol. Energy Mater. Sol. Cells*, vol. 156, pp. 85-92, 1998.

[12] J. F. Pierson, A. Thobor-Keck, and , and A. Billard, "Cuprite, paramelaconite and tenorite films deposited by reactive magnetron sputtering," *Appl. Surf. Sci*., vol. 1210, pp. 359-367, 2003.

[13] P. E. D. Morgan, D. E. Partin, B. L. Chamberland, and M. O'Keeffe, "Synthesis of Paramelaconite: Cu_4O_3," *J. Solid State Chem*., vol. 1121, pp. 33-37, 1996.

[14] D. Wu, Q. Zhang, and M. Tao, "LSDA+U study of cupric oxide: Electronic structure and native point defects," *Phys. Rev. B*, vol. 173, p. 235206, 2006.

[15] N. A. M. Shanid and M. A. Khadar, "Evolution of nanostructure, phase transition and band gap tailoring in oxidized Cu thin films," *Thin Solid Films*, vol. 1516, pp. 6245-6252, 2008.

[16] W. Ching, Y. N. Xu, and K. Wong, "Ground-state and optical properties of Cu_2O and CuO crystals," *Phys. Rev. B*, vol. 140, pp. 7684, 1989.

[17] A. A. Ogwu, E. Bouquerel, O. Ademosu, S. Moh, E. Crossan, and F. Placido, "The influence of rf power and oxygen flow rate during deposition on the optical transmittance of copper oxide thin films prepared by reactive magnetron sputtering," *J. Phys. D. Appl. Phys*., vol. 138, pp. 266-271, 2005.

[18] A. H. Jayatissa, K. Guo, and A. C. Jayasuriya, "Fabrication of cuprous and cupric oxide thin films by heat treatment," *Appl. Surf. Sci.*, vol. 1255, pp. 9474-9479, 2009.

[19] S. Ghosh, D. K. Avasthi, P. Shah, V. Ganesan, A. Gupta, D. Sarangi, R. Bhattacharya, and W. Assmann, "Deposition of thin films of different oxides of copper by RF reactive sputtering and their characterization," Vacuum, vol. 157, pp. 377-385, 2000.

[20] A. S. Reddy, G. V. Rao, S. Uthanna, and P. S. Reddy, "Structural and optical studies on dc reactive magnetron sputtered Cu_2O films," *Mater. Lett.*, vol. 160, pp. 1617-1621, 2006.

[21] A. Parretta, M. K. Jayaraj, A. D. Nocera, S. Loreti, L. Quercia, and A. Agati, "Electrical and optical properties of copper oxide films prepared by reactive RF magnetron sputtering," *Phys. Status Solidi A*, vol. 155, pp. 399-404, 1996.

[22] H. Zhu, J. Zhang, C. Li, F. Pan, T. Wang, and B. Huang, "Cu_2O thin films deposited by reactive direct current magnetron sputtering," *Thin Solid Films*, vol. 1517, 2009, pp. 5700-5704.

[23] S. C. Ray, "Preparation of copper oxide thin film by the sol–gel-like dip technique and study of their structural and optical properties," *Sol. Energy Mater. Sol. Cells*, vol. 168, pp. 307-312, 2001.

[24] M. Izaki, M. Nagai, K. Maeda, F. B. Mohamad, K. Motomura, J. Sasano, T. Shinagawa, and S. Watase, "Electrodeposition of 1.4-eV-Bandgap p-Copper (II) Oxide Film With Excellent Photoactivity," *J. Electrochem. Soc.*, vol. 1158, pp. D578-D584, 2011.

[25] J. B. Liang, N. Kishi, T. Soga, T. Jimbo, and M. Ahmed, "Thin cuprous oxide films prepared by thermal oxidation of copper foils with water vapor," *Thin Solid Films*, vol. 1520, pp. 2679-2682, 2012.

[26] A. M. El. Sayed and M. Shaban, "Structural, optical and photocatalytic properties of Fe and (Co, Fe) co-doped copper oxide spin coated films," *Spectrochim Acta A Mol and Biomol Spectrosc*, vol. 1149, no. 7, pp. 638-646, 2015.

[27] Y. Zhang, L. Pan, Y. Gu, and F. Zhao, "Metal-insulator transition in ferromagnetic Mn-doped CuO thin films," *J Appl Phys.*, vol. 1105, no. 8, pp. 086103, 2009.

[28] L. M. Walter, and J. W. Morse, "Reactive surface area of skeletal carbonate during dissolution: Effect of grain size," *J. Sediment. Petrol.*, vol. 154, pp. 1081–1090, 1984.

[29] G. Reisel and R. B. Heimann, "Correlation between surface roughness of plasma-sprayed chromium oxide coatings and powder grain size distribution: a fractal approach," *Surf. Coat. Technol*., vol. 1185, pp. 215–221, 2004.

[30] K. M. Elsabawy, W. F. EL-Hawary, and A. El-Maghraby, "Stability parameters and crystal visualization studies of anti-degradable cobalt cyclotetraphosphates for bone applications," *Int. J. Res. Environ. Sci. (IJRES)*, vol. 11, pp. 11–19, 2015.

[31] R. N. Mariammal, K. Ramachandran, G. Kalaiselvan *et al*., "Effect of magnetism on the ethanol sensitivity of undoped and Mn-doped CuO nanoflakes," *Appl. Surf. Sci*., vol. 1270, no. 4, pp. 545-552, 2013.

[32] X. G. Chen, W. W. Li, J. D. Wu, J. Sun, K. Jiang, Z. G. Hu, and J. H. Chu, "Temperature dependence of electronic band transition in Mn-doped SnO_2 nanocrystalline films determined by ultraviolet-near-infrared transmittance spectra," *Mater. Res. Bull*., vol. 147, pp. 111–116, 2012.

[33] J. L. Cai, and H. Gong, "The influence of Cu/Al ratio on properties of chemical vapor deposition grown p-type Cu–Al–O transparent semiconducting films[J]," *J Appl Phys*., vol. 198, no. 3, pp. 033707-033707-5, 2005.

[34] S. Ishizuka, S. Kato, T. Maruyama *et al*., "Nitrogen doping into Cu_2O thin films deposited by reactive radio-frequency magnetron sputtering," *Japanese Journal of Applied Physics*., vol. 140, no. 4, pp. 222-226, 2001.

[35] Z. Zang, A. Nakamura, and J. Temmyo, "Nitrogen doping in cuprous oxide films synthesized by radical oxidation at low temperature," *Mater Lett.*, vol. 192, pp. 188-191, 2013.

[36] N. M. Basith, J. J. Vijaya, L. J. Kennedy *et al.*, "Structural, optical and room-temperature ferromagnetic properties of Fe-doped CuO nanostructures," *Phys E.*, vol. 153, no. 53, pp. 193-199, 2013.

[37] Y. Gulen, F. Bayansal, B. Sahin *et al.*, "Fabrication and characterization of Mn-doped CuO thin films by the SILAR method," *Ceram Int*., vol. 139, no. 6, pp. 6475-6480, 2013.

An-Tian Du was born in Binzhou, Shandong province on November 30, 1993. He is a under graduate student, he majored in condensed matter physics of Yanbian University. His main research direction is functional material physics.

Guang-Rui Gu is a professor of Yanbian University. His main research interests are manganese oxide nanomaterials, nanostrcture carbon films, transparent conductive films and transition metal nitride/oxide films.

His main publications are: G. R. Gu and T. Ito, "Field emission characteristics of thin-metal-coated nano-sheet carbon films," *Applied Surface Science*, vol. 257, no. 7, pp. 2455-2460, 2011; L. L. Lan, G. R. Gu *et al*., "Manganese oxide nanostructures: Low-temperature selective synthesis and thermal conversion," *RSC Adv*., vol. 5, pp. 25250–25257, 2015; B. Xu, X. G. Ren G. R. Gu *et al*., "Structural and optical properties of Zn-doped SnO_2 films prepared by DC and RF magnetron co-sputtering," *Superlattices and Microstructures*, vol. 89, pp. 34-42, 2016.